Force-free current sheets in the Jovian magnetodisk: the key role of electron field-aligned anisotropy

A. V. Artemyev [1], **Q. Ma**[2,3], **R. W. Ebert** [4,5], **X.-J. Zhang**[6,1], **F. Allegrini**[4,5]

[1]Department of Earth, Planetary, and Space Sciences, University of California, Los Angeles, USA
[2]Department of Atmospheric and Oceanic Sciences, University of California, Los Angeles, CA, USA
[3]Center for Space Physics, Boston University, Boston, MA, USA
[4]Southwest Research Institute, San Antonio, TX, USA
[5]Department of Physics and Astronomy, University of Texas at San Antonio, San Antonio, TX, USA
[6]Department of Physics, University of Texas at Dallas, Richardson, TX, USA

Key Points:

- We report Juno observations of thin anisotropic current sheets in the Jovian magnetodisk
- The contribution of electron streams to the current sheet stress balance is estimated
- We show force-free current sheet configuration supported by strong electron field-aligned currents

Corresponding author: Anton Artemyev, `aartemyev@igpp.ucla.edu`

Abstract

Current sheets are an essential element of the planetary magnetotails, where strong plasma currents self-consistently support magnetic field gradients. The current sheet configuration is determined by plasma populations that contribute to the current density. The most commonly investigated configuration is supported by diamagnetic cross-field currents of hot ions, typical for the magnetospheres of magnetized planets. In this study, we examine a new type of the current sheet configuration supported by field-aligned currents from electron streams in the Jovian magnetodisk. Such bi-directional streams increase the electron thermal anisotropy close to the firehose instability threshold and lead to strong magnetic field shear. The current sheet configuration supported by electron streams is nearly force-free, with $|\mathbf{B}| \approx const$ across the sheet. Using Juno plasma and magnetic field measurements, we investigate the internal structure of such current sheets and discuss possible mechanisms for their formation.

1 Introduction

Current sheets are observed in all planetary magnetotails, the night-side regions of stretched magnetic field lines. The configuration of magnetotails depends on characteristics of the planetary magnetic field interaction with solar wind (Bagenal, 1992; Bagenal & Murdin, 2000; Jackman et al., 2014; Khurana & Liu, 2018), but all magnetotails contain current sheets, spatially localized regions of strong plasma currents. Instabilities of such current sheets, either internally or externally driven, can result in the magnetic reconnection that further transforms the magnetic energy to the plasma heating and charged particle acceleration (e.g., Birn et al., 2012; Gonzalez & Parker, 2016; Sitnov et al., 2019). Among all the current sheets in space plasmas, the one in Earth's magnetotail has been most intensively investigated, where strong diamagnetic currents, predominantly carried by hot protons (with a small fraction of oxygen ions), support the magnetic field configuration and pressure balance self-consistently (see Schematic in Fig. 1(a) and Birn, Schindler, and Hesse (2004); Sitnov and Merkin (2016); Zelenyi et al. (2011); Artemyev and Zelenyi (2013); Lu et al. (2016)). The current sheet in Earth's magnetotail is characterized by large plasma $\beta \sim 100$ (β is the ratio of plasma and magnetic field pressures), which leads to the dominant role of cross-field currents, $j_\perp \gg j_\parallel$, in the current sheet configuration. The relative contribution of ions and electrons to $j_\perp$ depends on the polarization electric fields, $\mathbf{E}_\perp$ (Schindler & Birn, 2002; Schindler et al., 2012); thin (ion-kinetic-scale) current sheets are, therefore, mostly electron dominated (Hesse et al., 1998; Runov et al., 2006; Artemyev et al., 2009; Lu et al., 2019) due to the strong polarization electric field within (Zelenyi et al., 2010; Lu et al., 2016). However, in the Earth's magnetotail, there are two interesting exceptions that $j_\parallel$ can be appreciably large. First, in the near-Earth magnetotail, during the current sheet thinning (formation of thin current sheets during the substrom growth phase, see Birn, Dorelli, et al. (2004); Petrukovich et al. (2007); Hsieh and Otto (2015)) the spatial scale (thickness) of the current sheet can become smaller than the thermal proton gyroradius. In such sub-ion scale thin current sheets the proton pressure cannot be redistributed within sub-gyroradius scale. To establish the pressure balance, the intensified field-aligned electron currents form strong magnetic field shear, contributing to a (partially) force-free current sheet configuration with $j_\perp \leq j_\parallel$ (see Schematic in Fig. 1(b) and Nakamura et al. (2008); Artemyev et al. (2013); Artemyev, Angelopoulos, Liu, and Runov (2017)). Second, a similar, partially force-free current sheet configuration has been observed in the distant (lunar orbit) magnetotail (Xu et al., 2018) where plasma β can be as low as ~ 1, and plasma pressure is not sufficient to establish the pressure balance. This second force-free current sheet with low β is also typical in Mars (Artemyev, Angelopoulos, Halekas, et al., 2017; DiBraccio et al., 2015) and Venus (Rong et al., 2015) magnetotails occupied by cold planetary plasmas.
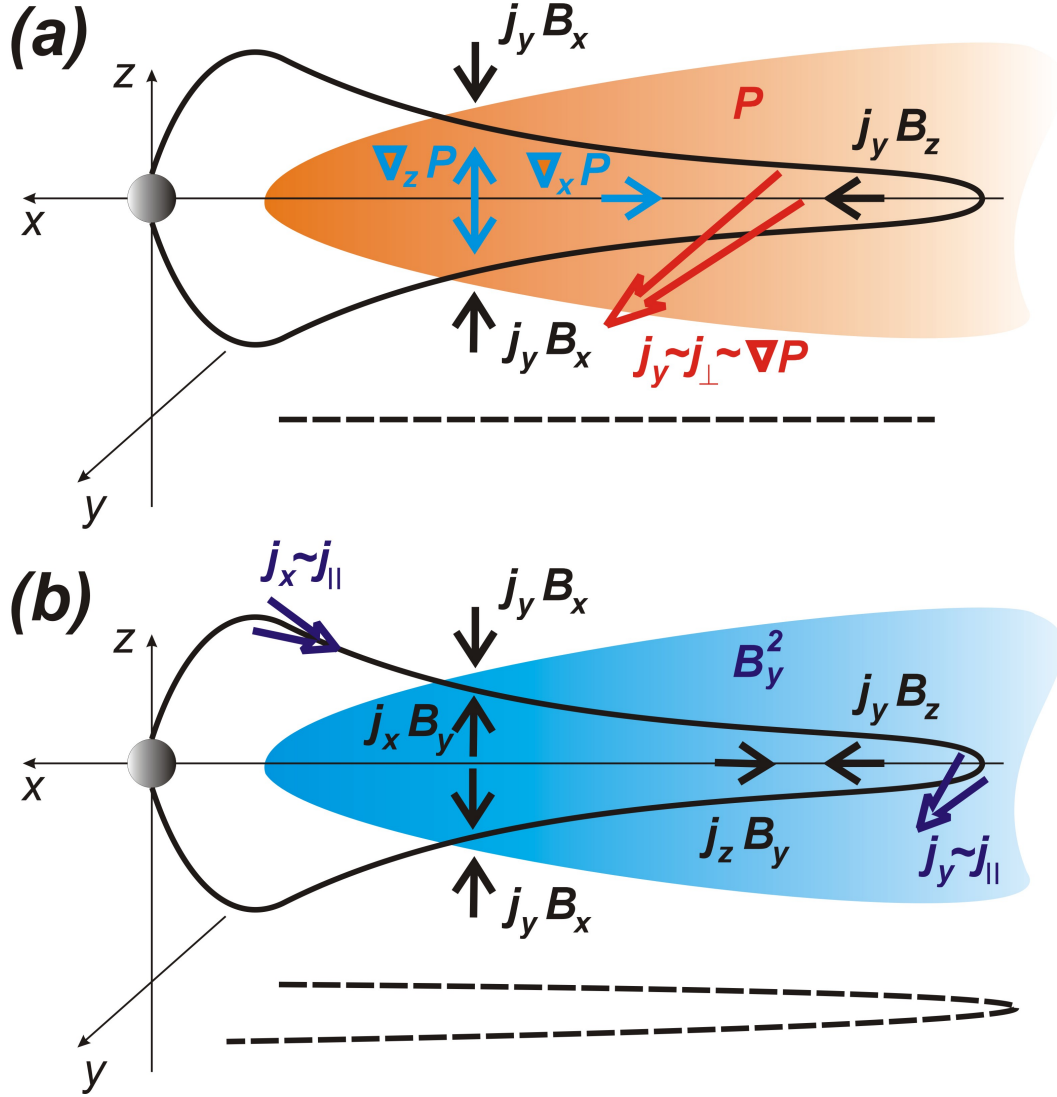
Figure 1. Schematic of current sheet configurations. (a) 2D configuration of the magnetic field line in the current sheet with plasma pressure P gradients (the dashed line parallel to the x-axis illustrates its projection to the xy plane). The main current density flows along the y-axis, transversely to magnetic field lines. (b) 3D configuration of the magnetic field line in the current sheet with $B_y^2/8\pi$ gradients playing the role of P gradients (see discussion on the $P \rightarrow B_y^2$ transition in Syrovatskii, 1981; Lukin et al., 2018). The dashed curve illustrates the field line projection to the xy plane. The main current density flows along $\mathbf{B}$, i.e., parallel to the magnetic field line.

Between the two mechanisms for the force-free (or partially force-free) current sheet formation, sub-ion scale thickness versus low plasma β, the first one is more interesting, because such sub-ion current sheets with strong field-aligned electron currents can be favorable to kinetically-driven magnetic field reconnection and current filamentation (Drake & Lee, 1977; Zelenyi & Taktakishvili, 1987; Wilson et al., 2016). Investigations of such current sheet configurations, however, are quite limited, because these current sheets are rather transient (dynamical) in the Earth's magnetotail (see discussions in Nakamura et al., 2008). An alternative plasma environment to investigate these specific current sheets would require hot heavy ions, curved magnetic field lines, and fast electron plasma flows. The best possible, accessible system is the Jovian magnetodisk, filled by sulfur and oxygen ions (Thomas et al., 2004; Krupp et al., 2004; Mauk et al., 2004; Kim et al., 2020a) with various charge states (e.g., Selesnick & Cohen, 2009; Clark et al., 2016; Allen et al., 2019; Kim et al., 2020b) and conjugate to the Jovian aroural region, a powerful source of field-aligned electron streams (e.g., Mauk et al., 2017b, 2017a). Therefore, We will use the recently available plasma and magnetic field measurements (Bagenal et al., 2017) from Juno in the Jovian magnetodisk to systematically examine sub-ion scale, force-free (or partially force-free) current sheets.

In this study, we focus on 18 events of Juno current sheet crossings during the first 30 orbits, i.e., those with a strong magnetic shear (field-aligned currents), electron field-aligned streams, and different combinations of proton and heavy ion contributions to the pressure. We estimate the current sheet spatial scale (thickness) and current density during its flapping motion. The following of paper includes three sections: description of Juno instruments and data analysis techniques in Sect. 2, detailed analysis of 9 current sheet crossings in Sect. 3, and discussion on the results in Sect. 4.

2 Data analysis technique and instruments

We use data from the Juno magnetometer (MAG) in 2017-2018, with 1s time resolution (Connerney, Benn, et al., 2017; Connerney, Adriani, et al., 2017). We focus on measurements at $r > 25R_J$ radial distances in the Jovian magnetodisk. Figure 2 shows a typical one-day magnetic field measurements in the magnetodisk by Juno: quasi-periodic crossings of zeros of the radial magnetic field component $B_r = 0$ (current sheet) are due to flapping oscillations of the magnetodisk. For each such crossing we transform the magnetic field into local coordinate systems (Sonnerup & Cahill, 1968): B_l is the most varying magnetic field component, B_n is the less varying component, and B_m is transverse to B_l and B_n. We keep only those current sheets with a B_m peak at $B_l = 0$ and with available plasma measurements by the Jovian Auroral Distributions Experiment (JADE) instrument. The times of selected crossings are given in table 1, along with their radial distances. Overview plots of plasma and magnetic field profiles during each current sheet crossing are provided in the Supporting Information. In the main text, we mostly discuss six force-free current sheets, in comparison with three current sheets supported by plasma pressure gradients (non-force-free sheets), but our conclusions are supported by the entire dataset.

Jovian Auroral Distributions Experiment (JADE) measures (see McComas, Alexander, et al., 2017; McComas, Szalay, et al., 2017; Kim et al., 2020a, 2020b) electron distributions from below ~ 0.1 to 100 keV (at a 1 s cadence) and ions from ~ 13 eV to ~ 50 keV (including ion composition, at a 1 s cadence). We have averaged JADE data over the spin period (30 s) to obtain a complete pitch angle coverage from $0°$ to $180°$. These energy ranges cover the main (thermal) plasma populations in Jupiter's magnetodisk. We use the following data products from JADE: electron pitch-angle/energy distributions averaged over time interval of the current sheet crossing, electron omni-directional energy spectra (energy flux) $F_e(t, E)$, electron pressure $p_e(t)$ and density $n_e(t)$ profiles, electron pressure anisotropy $A_e = p_{e,\parallel}/p_{e,\perp}$ averaged over the current sheet crossing interval, omnidirectional proton and heavy ion energy spectrum (energy
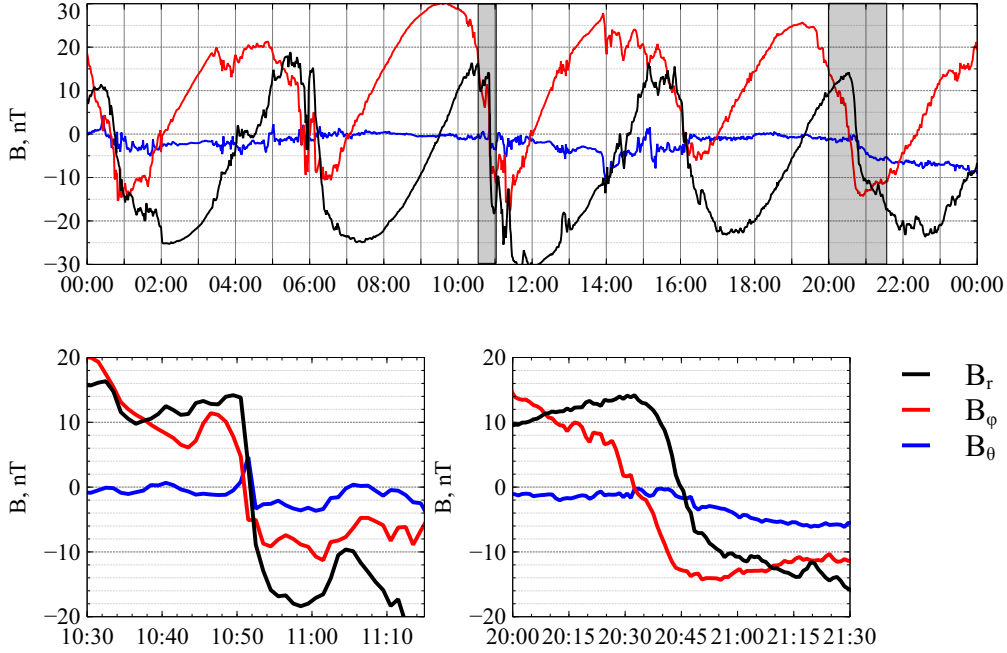
Figure 2. Top panel shows one-day measurements by Juno MAG: radial B_r, azimuthal B_φ, and north-south B_θ components. Bottom panels show the expanded view of two current sheet crossings from the top panel.

flux) $F_p(t, E)$ and $F_i(t, E)$, and proton and heavy ion densities $n_p(t)$, $n_i(t)$. Note that field view of the JADE electron detector may not cover the entire $[0, 180°]$ pitch-angle range at the current sheet boundaries, so we average electron measurements over each current sheet crossing interval to obtain a more complete pitch-angle distribution. The rotation of the background magnetic field direction across the current sheet ensures a wide coverage of the pitch-angle range (see pitch-angle distributions below), which is needed for the estimate of A_e. In this study, we use the *heavy ion* (or "i") to denote integrated quantities of those ion populations with mass-to-charge ratio larger than five. We also estimate proton and heavy ion pressures $p_p(t)$, $p_i(t)$ as moments of the omnidirectional energy spectrum, i.e., we assume that thermal proton and ion speeds well exceed their bulk flow speed (this is a reasonable assumption, see Kane et al., 1999; Frank et al., 2002; Waldrop et al., 2005; Kim et al., 2020b).

Using plasma and magnetic field measurements, we estimate $\beta_{e,p,i} = 8\pi p_{e,p,i}/B^2$ profiles and electron fire-hose parameter $\Lambda_e \approx \beta_e(A_e - 1)/2 = 4\pi(p_{\parallel e} - p_{\perp e})/B^2$. To show that this parameter controls the contribution of the electron anisotropy to the current density, we illustrate the case for a simple quasi-1D current sheet with $\partial B_l/\partial r_n = 4\pi j_m/c$, $\partial B_m/\partial r_n = 4\pi j_l/c$, and $B_n = const \neq 0$. The electron current due to cross-field drifts in such current sheet is (Shkarofsky et al., 1966)

$$\mathbf{j}_{\perp e} = -ecn\frac{[\mathbf{E} \times \mathbf{B}]}{B^2} - c\frac{[\nabla p_{\perp e} \times \mathbf{B}]}{B^2} + \frac{c\Lambda_e}{4\pi}\frac{[\mathbf{B} \times (\mathbf{B}\nabla)\mathbf{B}]}{B^2} \tag{1}$$

where $\mathbf{E}_\perp$ is the transverse component of the polarization electric field. This equation should be supplemented by the field-aligned stress balance equation

$$enE_\parallel = -\nabla_\parallel p_{\parallel e} + \frac{\Lambda_e}{4\pi}(\mathbf{B}\nabla)B$$

#	date	time	radial distance	comments
1	2017 doy 027	09:00-09:20	$65R_J$	ff CS, heavy ions
2	2017 doy 080	07:10-07:40	$61R_J$	ff CS, heavy ions
3	2017 doy 080	17:10-17:50	$61R_J$	non-ff CS, heavy ions
4	2017 doy 128	08:00-08:30	$86R_J$	ff CS, heavy ions
5	2017 doy 128	16:30-17:30	$86R_J$	ff CS, heavy ions
6	2017 doy 133	05:10-06:10	$61R_J$	non-ff CS, heavy ions
7	2017 doy 181	06:50-07:20	$86R_J$	ff CS, heavy ions
8	2017 doy 181	09:45-10:20	$86R_J$	ff CS, heavy ions
9	2018 doy 031	09:30-10:40	$50R_J$	non-ff CS, heavy ions
10	2018 doy 034	13:30-14:30	$50R_J$	non-ff CS, heavy ions
11	2018 doy 085	21:00-21:50	$62R_J$	non-ff CS, protons
12	2018 doy 086	10:15-11:15	$55R_J$	ff CS, heavy ions & protons
13	2018 doy 088	01:20-02:30	$38R_J$	ff CS, protons
14	2018 doy 088	11:30-12:30	$38R_J$	ff CS, protons
15	2018 doy 088	21:30-22:30	$38R_J$	ff CS, heavy ions
16	2018 doy 141	10:30-11:15	$38R_J$	ff CS, heavy ions & protons
17	2018 doy 141	19:45-21:00	$38R_J$	ff CS, heavy ions & protons
18	2018 doy 142	20:00-20:45	$26R_J$	non-ff CS, heavy ions & protons

Table 1. List of current sheet crossings. In the comments column, ff CS and non-ff CS stand for the force-free and non force-free current sheets, respectively. The dominant ion type (heavy ions or protons) is also indicated in the comments column.

where $E_\parallel$ is the field-aligned component of the polarization electric field and $\nabla_\parallel = (\mathbf{B}/B)\nabla$.

For force-free current sheets with $\nabla_n p_{e\perp} = \nabla_n p_{e\parallel} = \nabla_n B = 0$, the current density equation can be rewritten as

$$\mathbf{j}_{\perp e} = \frac{c\Lambda_e}{4\pi}\left(-\mathbf{e}_l\frac{B_n^2}{B^2}\nabla_n B_m + \mathbf{e}_m\frac{B_n^2}{B^2}\nabla_n B_l + \mathbf{e}_n\frac{B_n}{B^2}\left(B_l\nabla_n B_m - B_m\nabla_n B_l\right)\right)$$

whereas the parallel current density can be obtained from the divergence free condition:

$$j_{\parallel e} = -\frac{1}{B}\left(B_l\nabla_n B_m - B_m\nabla_n B_l\right)$$

Thus, the total electron current is

$$
\begin{aligned}
\mathbf{j}_e &= \mathbf{j}_{\perp e} + j_{\parallel e}\frac{\mathbf{B}}{B} = 4\pi c\Lambda_e\left(-\mathbf{e}_l\left(\nabla_n B_m - \frac{B_m\nabla_n B}{B}\right) + \mathbf{e}_m\left(\nabla_n B_l - \frac{B_m\nabla_n B}{B}\right)\right) \\
&= \frac{c\Lambda_e}{4\pi}\left(-\mathbf{e}_l\nabla_n B_m + \mathbf{e}_m\nabla_n B_l\right) = \Lambda_e\mathbf{j}
\end{aligned}
\tag{2}
$$

where $\mathbf{j} = (c/4\pi)\nabla\times\mathbf{B}$.

3 Current sheet examples

Figure 3 shows six typical examples of thin current sheets with an almost constant magnetic field magnitude across the sheet, $|\mathbf{B}| \approx const$. Such a constant magnetic field implies the dominant role of field-aligned currents in the current sheet configuration: if $\mathbf{j} = C\cdot\mathbf{B}$, then $\mathbf{j}\times\mathbf{B} = 0$ and there is no pressure variation across the sheet (note

that typical crossings of the magnetodisk current sheet show strong variations of the plasma pressure (density) across the sheet, see, e.g., Huscher et al., 2021). Panels (a) show that $|\mathbf{B}| = const$ is due to peak of B_m component that compensates the drop of B_l^2 around the neutral plane (where $B_l = 0$). As expected for the force-free current sheet, there are no appreciable variations in the ion fluxes (protons or heavy ions) across the sheet (see panel (c)). Electron fluxes may show some variations (see panel (b)), but variations of the electron thermal pressure are insufficient to cause any significant variations of the magnetic field pressure (see panel (d); note that a variation of $10^{-2} \cdot cm^{-3}$keV corresponds to ≈ 2nT variation of the magnetic field).

Let us explain the absence of ion pressure variations during the observed current sheet crossings. As shown in Fig. 3, the time-scale of current sheet crossings varies from $T \sim 5$ min to 30 min; taking into account the flapping speed of $\sim \omega_J R \tan\theta$, this time-scale can be converted to a spatial scale $L \approx 1000$km$\cdot(r/50R_J)\cdot(T/60$s$) \in [5, 30]\cdot 10^3 km$ (here ω_J is the Jupiter rotational frequency, r is the radial distance of the current sheet, and $\theta \approx 9.5°$ is the tilt angle of the magnetodisk with respect to the planetary equator, see Connerney et al. (1998); Khurana and Schwarzl (2005)). Despite that we used the upper limit for the flapping speed (see discussion and observations in Hill, 1979; Kim et al., 2020b), this spatial scale is much smaller than the typical thicknesses of Jovian magnetodisk current sheets, $L \sim 2R_J \approx 10^5$km (Connerney et al., 2020; Liu et al., 2021; Khurana et al., 2022). More importantly, this spatial scale is comparable to (or smaller than) the hot proton or heavy ion gyroradius: for the equatorial field of a typical current sheet, ~ 5nT, ~ 30keV protons and sulfur ions have gyroradii of ~ 5000km and ~ 25000km, respectively. Thus, these current sheets are likely on sub-ion scale, within which ions cannot redistribute their pressure. To establish the pressure balance in such current sheets, the field-aligned electron currents create a local B_m peak.

To estimate the electron contribution to the field-aligned currents, we use Eq. (2) and the measured electron pitch-angle, energy distributions. Figure 4(b) shows that all six current sheets are characterized by field-aligned bi-directional electron streams. These streams occupy $\sim 30°$ in pitch angles around the parallel and anti-parallel (with respect to the background magnetic field) directions, in the energy range below ~ 10 keV. Such field-aligned streams may be generated by reconnection further downtail (e.g., Kronberg et al., 2012) or originate from the aurora acceleration region (Mauk et al., 2017b, 2020; Elliott et al., 2020; Allegrini et al., 2020). In the Earth's magneto-sphere, similar field-aligned streams are observed in the near-Earth magnetotail (Hada et al., 1981; Walsh et al., 2013; Artemyev, Angelopoulos, Liu, & Runov, 2017), but their energies are well below ~ 1keV, in agreement with the capability of the Earth's aurora acceleration (Ergun et al., 2004; Chaston et al., 2007; Watt & Rankin, 2009). More effective aurora acceleration in the Jupiter magnetosphere may produce ~ 10 keV beams (Kollmann et al., 2018; Saur et al., 2018; Damiano et al., 2019; Lysak et al., 2021), which are likely further expanded in the pitch-angle space by various scattering mechanisms and form the electron streams observed in the plasma sheet (see discussion in Zhang et al., 2020). In the presence of a large electron $\beta_e \sim 1$, such field-aligned streams create a strong pressure anisotropy with the fire-hose parameter Λ_e reaching one (see Fig. 4(c)). Thus, Eq. (2) shows that for this large Λ_e, electrons will carry almost all the current to support B_l and B_m variations across the sheet.

We explain the formation of force-free (partial force-free) current sheets with strong field-aligned electron currents (shown in Fig. 4) as a need to balance the magnetic field pressure decrease $\sim B_l^2$ on a sub-ion scale. This explanation implies that similar electron currents should be observed in current sheets on larger scales, where they will not create B_m peaks, but rather contribute to the cross-field current density, in agreement with Eq. (1) (see discussion in Artemyev et al., 2016). Figure 5 shows such current sheets with a significant ion pressure contribution to the stress
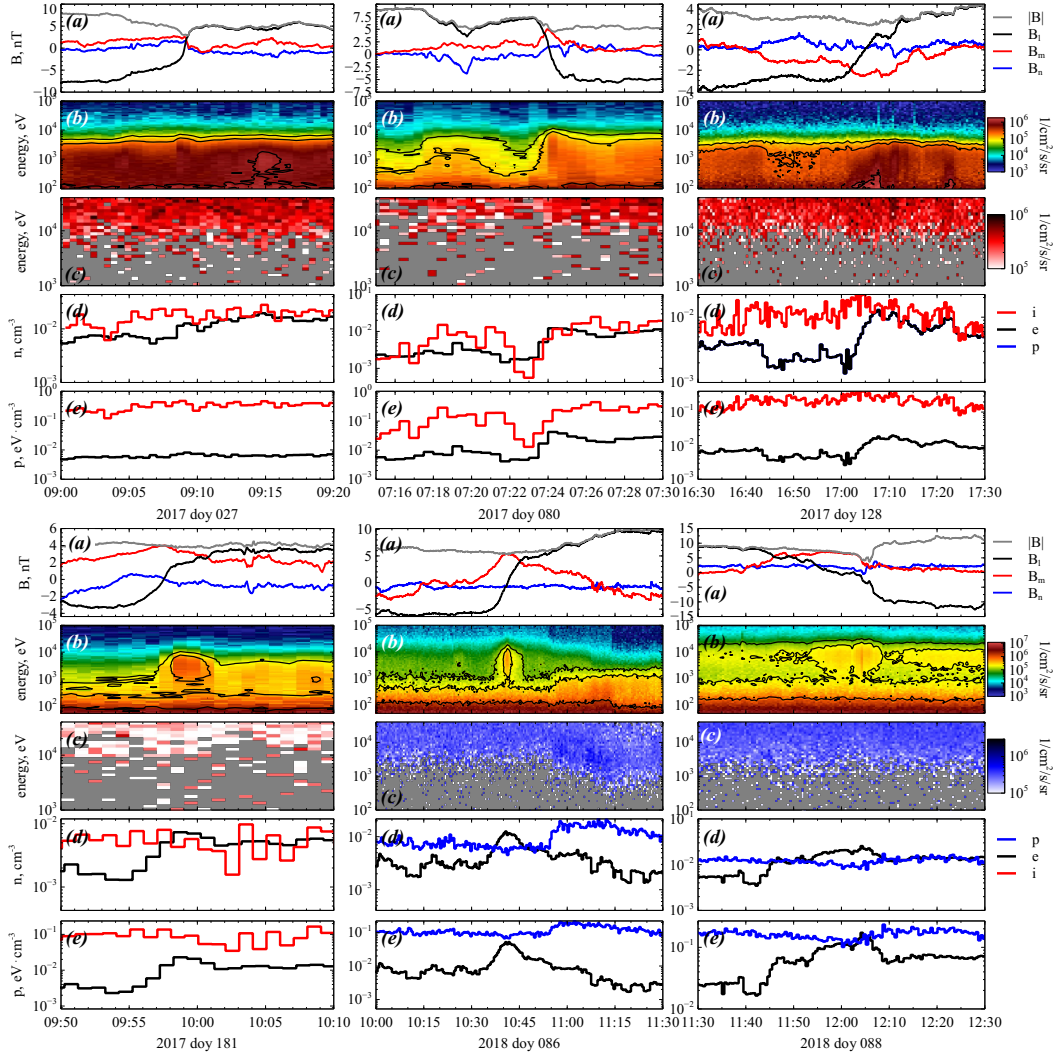
Figure 3. Six examples of force-free current sheets observed by Juno in different radial distances (see table 1). (a) Magnetic field components in the local (MVA) coordinate system and the magnetic field magnitude. (b, c) Omnidirectional spectra of electrons and dominant ion species (blue for protons and red for heavy ions). (d,e) Densities and pressures of electrons and dominant ion species.
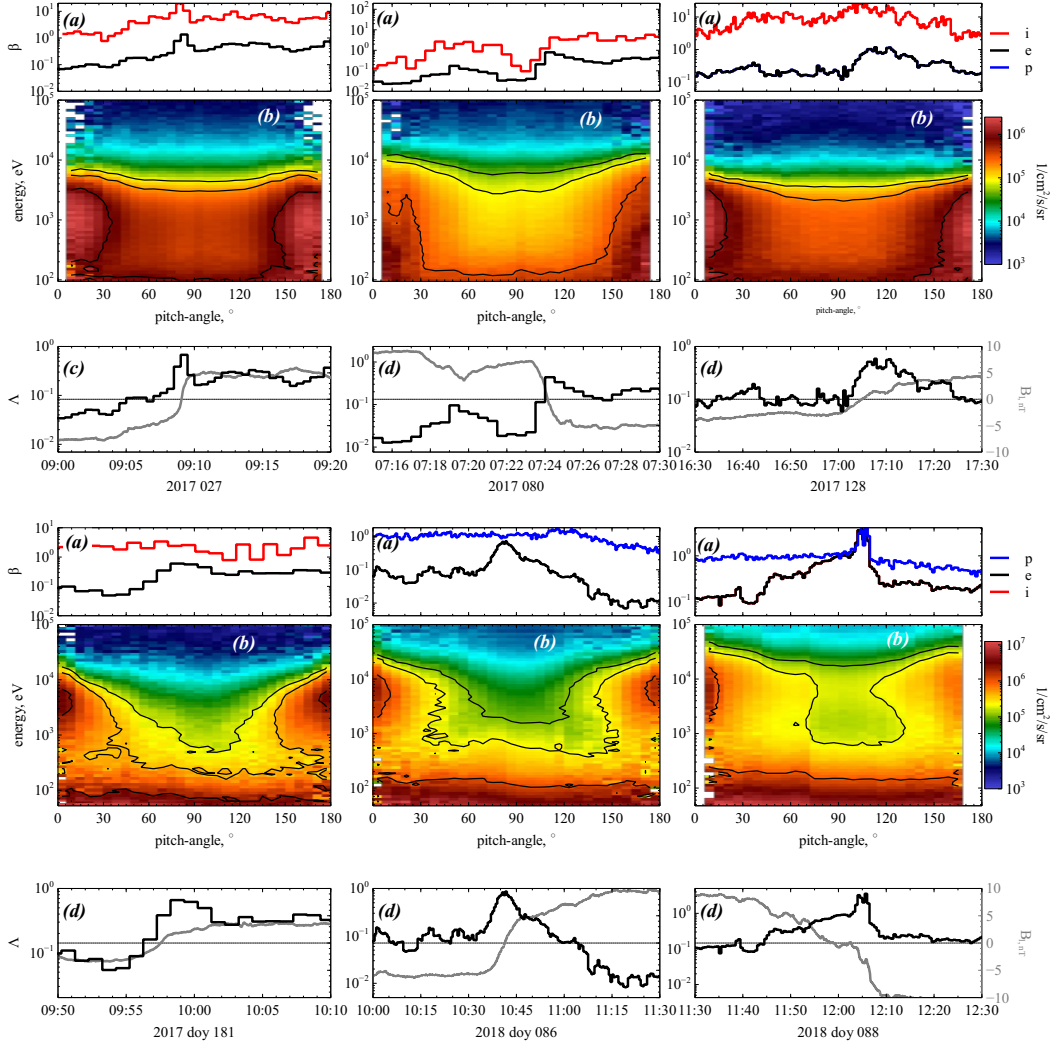
Figure 4. Six examples of force-free current sheets from Fig. 3. (a) Electron and ion betas. (b) Electron pitch-angle, energy distribution averaged over the entire event. (c) Electron fire-hose parameter and B_l field to illustrate the current sheet center.

balance and strong field-aligned electron anisotropy. There is almost no B_m peak in the current sheet center (where $B_l \sim 0$, see panel (a)), whereas ion fluxes and pressures exhibit peaks (panels (c,d)). Temporal scales of current sheet crossings from Fig. 5 are about 20-30min, corresponding to a spatial scale larger than the typical proton and heavy ion gyroradius in these current sheets. Note the two current sheets on 2017 doy 080 (shown in Fig. 3 and 5) exhibit different characteristics: the force-free current sheet in Fig. 3 was crossed within a couple of minutes and shows no p_i variations, whereas the one in Fig. 5 was crossed within ~ 15 min and shows strong p_i variations.

In current sheets from Fig. 5, electron pitch-angle distributions contain strong field-aligned streams with characteristics very similar to those in the force-free current sheets (compare Figs. 4(b) and 5(g)). However, contrary to force-free current sheets, these field-aligned streams mostly contribute to anisotropic cross-field electron currents, see Eq. (1). Indeed, small magnetic field pressure at the current sheet center (where $B_l \sim 0$) increases β_e and leads to a large electron fire-hose parameter $\Lambda_e \approx 1$ even for a moderate anisotropy A_e (see Fig. 5(f,h)).

Comparison of Figs. 3, 4, and 5 suggests the following mechanism for the formation of the force-free current sheet. Certain external conditions (e.g., electron acceleration in the aurora region, see Mauk et al. (2017b); Saur et al. (2018); Damiano et al. (2019); Lysak et al. (2021)) generate field-aligned electron streams bouncing within the current sheet in the Jovian magnetodisk. These streams contribute to the field-aligned electron anisotropy, $A_e > 1$, and fire-hose parameter $\Lambda_e > 0$. In typical thick current sheets such anisotropy supports the cross-field electron currents (see Eq.(1)) and may create a thin, sub-ion scale current sheet embedded into a thick, ion scale current sheet (e.g., Zelenyi et al., 2004; Mingalev et al., 2018; Kamaletdinov et al., 2020; Zelenyi et al., 2022). Indeed, the magnetic field profiles in Fig. 5 exhibit stronger gradients around $B_l \sim 0$. If external drivers result in the current sheet thinning, the current sheet may reach sub-ion spatial scale where ions cannot redistribute their pressure and maintain the stress balance. In this case, the electron currents form B_m peaks to balance the B_l^2 drop at the current sheet center, and self-consistently evolve from the cross-field currents to field-aligned currents (see Schematic in Fig. 1).

4 Discussion

In this study, we investigate force-free (and partially force-free) current sheets, where field-aligned electron streams support the pressure anisotropy and parallel currents, leading to the formation of the B_m peak at the current sheet center, $B_l = 0$. Let us discuss the difference of the stress balance in such current sheets from that in more typical *thick* current sheets. In current sheets, the 2D stress balance in the equatorial plane (balance along the radial direction) is maintained by a combination of the centrifugal force, plasma pressure force, and magnetic field line tension force (Hill & Carbary, 1978; Cheng, 1983; Zimbardo, 1989):

$$\frac{1}{c}j_\varphi B_\theta + m_i n \omega_J^2 r + \nabla_r \hat{p} = 0 \tag{3}$$

where $\nabla_r \hat{p}$ is the radial component of the plasma pressure tensor gradient. In the local coordinate system, $\mathbf{l} \approx \mathbf{e}_r$ and $\mathbf{m} \approx \mathbf{e}_\phi$. Based on the vertical stress balance, $8\pi p = \max B_l^2 - \max B_m^2$, we may estimate the current density as:

$$j_m \approx \frac{c}{4\pi} \frac{\max B_l}{B_n} \nabla_r \max B_l \approx 5.5 \frac{\text{nA}}{\text{m}^2} \cdot (r/R_J)^{-2} \approx 12 \frac{\text{pA}}{\text{m}^2} \cdot \left(\frac{r}{30R_J}\right)^{-2} \tag{4}$$

where $\max B_l \approx 50\text{nT} \cdot (r/R_J)^{-1}$ and $\max B_l/B_n \approx 20$ are the empirical relations (see, e.g., Artemyev et al., 2014; Liu et al., 2021). The corresponding current sheet thickness $L = c \max B_l/4\pi j_m \approx 1.5R_J \cdot (r/30R_J)^{-1}$ should be larger than $1R_J$ at $r > 30R_J$, which is consistent with the thickness estimates for typical *thick* current sheets (e.g.,
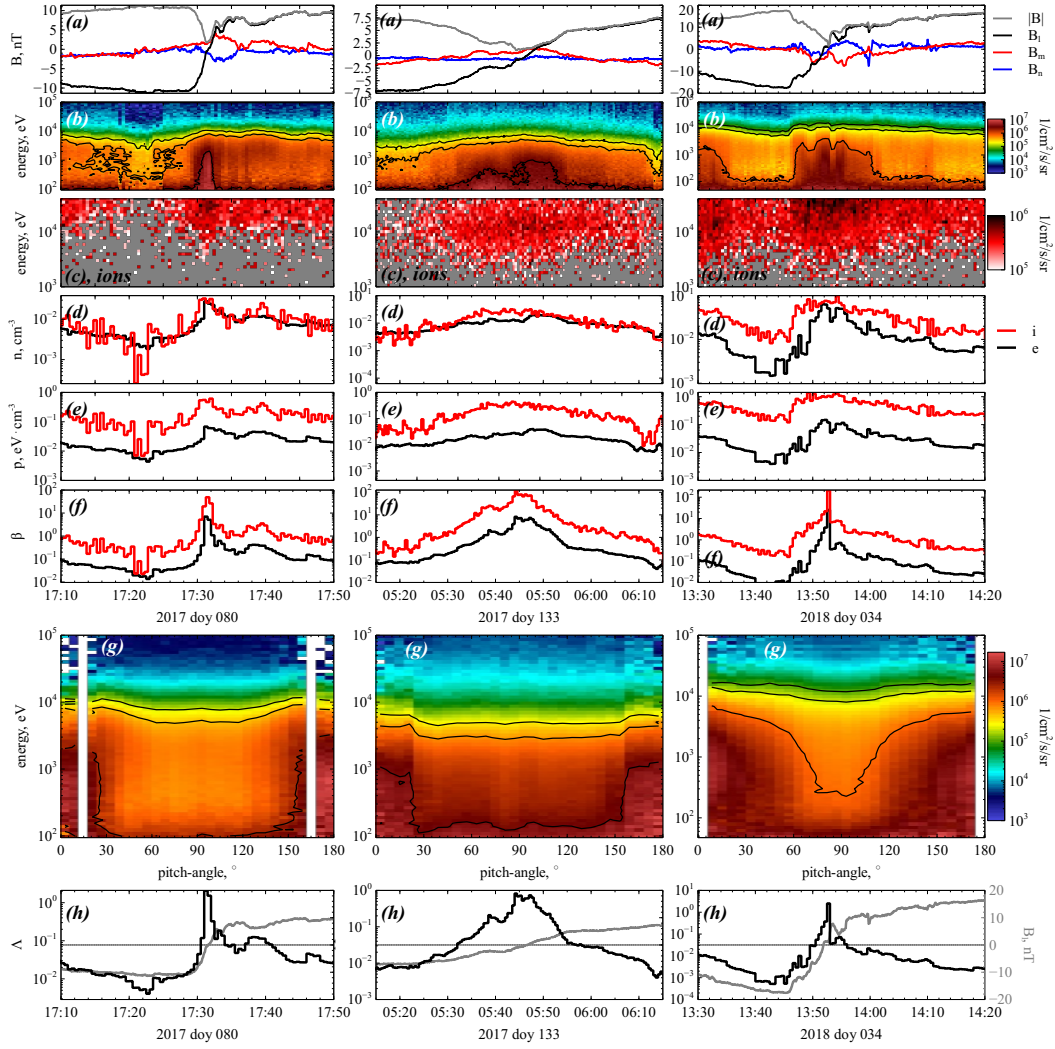
Figure 5. Three examples of current sheets with large field-aligned electron currents and plasma pressure variations observed by Juno in different radial distances (see table 1). (a) Magnetic field components in the local (MVA) coordinate system and the magnetic field magnitude. (b, c) Omnidirectional spectra of electrons and dominant ion species. (d, e) Densities and pressures of electrons and dominant ion species. (f) Electron and ion beta. (g) Electron pitch-angle and energy distribution averaged over the entire event. (h) Electron fire-hose parameter and B_l field to show the current sheet center.

Khurana et al., 2004; Liu et al., 2021). Such current sheets will be crossed during an interval of $\Delta t = L/\omega_j r \tan\theta \approx 3\text{hours} \cdot (r/30R_J)^{-2}$; for much thinner current sheets as in our dataset, the traversal timescale will be less than 10 min (see Fig. 3). The stress balance in such thin current sheets cannot be maintained by centrifugal force and radial gradient of the plasma pressure. Instead, the electron pressure anisotropy contributes to the stress balance (Rich et al., 1972):

$$\nabla_r \hat{p} = \nabla_r p_\perp + \nabla_\theta \frac{p_{\|e} - p_{\perp e}}{B^2} B_r B_\theta \approx \nabla_\theta \left(\frac{\Lambda_e}{4\pi} B_r B_\theta \right) \tag{5}$$

This equation shows that the thin current sheet configuration resembles a classical rotational discontinuity, with no variations of the Alfven speed because of the pressure anisotropy (Hudson, 1970):

$$\Delta v_A = \sqrt{\frac{B^2}{4\pi n m_i} \left(1 - \Lambda_e \right)} \sim 0 \tag{6}$$

This condition allows for a balance of the 1D current sheet (with thickness L much smaller than the spatial scale of the radial gradient of the plasma density) without fast plasma flows typical for rotational discontinuities in anisotropic plasma, where cross-sheet change of the plasma flow velocity equals to Δv_A (see discussions of the anisotropy contribution to the force-free current sheet configurations in Vasko et al., 2014; Artemyev, Angelopoulos, Vasko, & Zelenyi, 2020). Formation of such 1D current sheets around the fire-hose marginally stability threshold has been predicted theoretically (e.g., Francfort & Pellat, 1976; Cowley, 1978; Cowley & Pellat, 1979), but never have been detected under quiet geomagnetic conditions in the Earth's magnetotail (see discussion in Sitnov et al., 2006; Artemyev & Zelenyi, 2013). Observations of these current sheets in the Jovian magnetotail confirm the theoretical predictions, which can further lead to improved current sheet models (see discussion on development of the next generation of current sheet models in Sitnov & Merkin, 2016; Y. D. Yoon et al., 2021; Zelenyi et al., 2022).

It is worth to note that these current sheets are electromagnetically *disconnected* from the Jovian ionosphere, because the local Alfven speed is zero, $v_A = (B/\sqrt{4\pi n m_i}) \cdot \sqrt{1 - \Lambda_e} = 0$, and there are no field-aligned perturbations propagating from the current sheet to the ionosphere. Such local destruction of magnetosphere-ionosphere coupling is an interesting phenomenon that we do not observe in the Earth's magnetotail, where Λ_e is much more moderate (Artemyev, Angelopoulos, Vasko, Petrukovich, et al., 2020).

Theoretical investigations of these force-free current sheets in the Jovian magnetodisk is a real challenge for plasma kinetics, because these current sheets share properties of 2D plasma equilibria (with the tension force $\sim (4\pi/c) \cdot j_m B_n$) and properties of rotational discontinuities (with $\mathbf{j} = C \cdot \mathbf{B}$ and $B_n \neq 0$). All existing 2D kinetic current sheet models operate with the plasma pressure gradients, $\nabla p = c^{-1} \mathbf{j} \times \mathbf{B}$, and do not include field-aligned currents (see, e.g., P. H. Yoon & Lui, 2005; Vasko et al., 2013; Zelenyi et al., 2011; Sitnov et al., 2006; Sitnov & Merkin, 2016, and references therein). Existing models of force-free current sheets mostly assume 1D tangential discontinuities with $B_n = 0$ (see, e.g., Harrison & Neukirch, 2009; Panov et al., 2011; Neukirch, Vasko, et al., 2020; Neukirch, Wilson, & Allanson, 2020, and references therein). Construction of the kinetic model for 1D rotational discontinuities requires assumptions of an additional system symmetry (e.g., Sonnerup & Su, 1967; Artemyev, 2011; Mingalev et al., 2012; Vasko et al., 2014), whereas kinetic models of 2D rotational discontinuities have not yet been constructed. Although fluid models of 2D rotational discontinuities (with $\mathbf{j} = C \cdot \mathbf{B}$, $j_n B_m = j_m B_n$, and $B_n \neq 0$) can be constructed (e.g., Cowley, 1978; Hilmer & Voigt, 1987; Hau & Voigt, 1992; Lukin et al., 2018), their kinetic realization has not been demonstrated. Therefore, further theoretical investigations are needed to explain Juno observations in the Jovian magnetodisk.

5 Conclusions

We have investigated thin (thickness is smaller than or about the hot ion gyroradius) current sheets observed by Juno in the Jovian magnetodisk and characterized by strong field-aligned electron streams. We have demonstrated that electron streams support the strong field-aligned anisotropy, which may increase the fire-hose parameter up to the instability threshold, $\Lambda_e = 4\pi(p_{e\parallel} - p_{e\perp})/B^2 \to 1$. In such thin, marginally stable current sheets, almost all current is field-aligned, and the current sheet configuration is force-free, with $\mathbf{j} \times \mathbf{B} \approx 0$. This is a new type of strongly anisotropic, force-free current sheets, which has not been reported in the quiet-time Earth's magnetopshere or solar wind. Further numerical investigations of such current sheet formation and dynamics will reveal their potential role in the particle acceleration (e.g., via magnetic reconnection).

Open Research

Data processing was done using SPEDAS V4.1, see Angelopoulos et al. (2019). All the adopted data are available in the archive `https://doi.org/10.5281/zenodo.7470240`

References

Allegrini, F., Mauk, B., Clark, G., Gladstone, G. R., Hue, V., Kurth, W. S., ... Wilson, R. J. (2020, April). Energy Flux and Characteristic Energy of Electrons Over Jupiter's Main Auroral Emission. *Journal of Geophysical Research (Space Physics)*, *125*(4), e27693. doi: 10.1029/2019JA027693

Allen, R. C., Paranicas, C. P., Bagenal, F., Vines, S. K., Hamilton, D. C., Allegrini, F., ... Wilson, R. J. (2019, Nov). Energetic Oxygen and Sulfur Charge States in the Outer Jovian Magnetosphere: Insights From the Cassini Jupiter Flyby. *Geophys. Res. Lett.*, *46*(21), 11,709-11,717. doi: 10.1029/2019GL085185

Angelopoulos, V., Cruce, P., Drozdov, A., Grimes, E. W., Hatzigeorgiu, N., King, D. A., ... Schroeder, P. (2019, January). The Space Physics Environment Data Analysis System (SPEDAS). *Space Sci. Rev.*, *215*, 9. doi: 10.1007/s11214-018-0576-4

Artemyev, A. V. (2011, February). A model of one-dimensional current sheet with parallel currents and normal component of magnetic field. *Physics of Plasmas*, *18*(2), 022104. doi: 10.1063/1.3552141

Artemyev, A. V., Angelopoulos, V., Halekas, J. S., Runov, A., Zelenyi, L. M., & McFadden, J. P. (2017, May). Mars's magnetotail: Nature's current sheet laboratory. *J. Geophys. Res.*, *122*, 5404-5417. doi: 10.1002/2017JA024078

Artemyev, A. V., Angelopoulos, V., Liu, J., & Runov, A. (2017, January). Electron currents supporting the near-Earth magnetotail during current sheet thinning. *Geophys. Res. Lett.*, *44*, 5-11. doi: 10.1002/2016GL072011

Artemyev, A. V., Angelopoulos, V., Vasko, I. Y., Petrukovich, A. A., Runov, A., Saito, Y., ... Strangeway, R. J. (2020, January). Contribution of Anisotropic Electron Current to the Magnetotail Current Sheet as a Function of Location and Plasma Conditions. *Journal of Geophysical Research (Space Physics)*, *125*(1), e27251. doi: 10.1029/2019JA027251

Artemyev, A. V., Angelopoulos, V., Vasko, I. Y., & Zelenyi, L. M. (2020, January).

Ion Nongyrotropy in Solar Wind Discontinuities. *Astrophys. J. Lett.*, *889*(1), L23. doi: 10.3847/2041-8213/ab6b2e

Artemyev, A. V., Petrukovich, A. A., Frank, A. G., Nakamura, R., & Zelenyi, L. M. (2013, June). Intense current sheets in the magnetotail: Peculiarities of electron physics. *J. Geophys. Res.*, *118*, 2789-2799. doi: 10.1002/jgra.50297

Artemyev, A. V., Petrukovich, A. A., Zelenyi, L. M., Nakamura, R., Malova, H. V., & Popov, V. Y. (2009, October). Thin embedded current sheets: Cluster observations of ion kinetic structure and analytical models. *Annales Geophysicae*, *27*, 4075-4087.

Artemyev, A. V., Vasko, I. Y., Angelopoulos, V., & Runov, A. (2016, September). Effects of electron pressure anisotropy on current sheet configuration. *Physics of Plasmas*, *23*(9), 092901. doi: 10.1063/1.4961926

Artemyev, A. V., Vasko, I. Y., & Kasahara, S. (2014). Thin current sheets in the Jovian magnetotail. *Planatary Space Science*, *96*, 133-145. doi: 10.1016/j.pss.2014.03.012

Artemyev, A. V., & Zelenyi, L. M. (2013). Kinetic Structure of Current Sheets in the Earth Magnetotail. *Space Sci. Rev.*, *178*, 419-440. doi: 10.1007/s11214-012-9954-5

Bagenal, F. (1992). Giant planet magnetospheres. *Annual Review of Earth and Planetary Sciences*, *20*, 289-328. doi: 10.1146/annurev.ea.20.050192.001445

Bagenal, F., Adriani, A., Allegrini, F., Bolton, S. J., Bonfond, B., Bunce, E. J., . . . Zarka, P. (2017, November). Magnetospheric Science Objectives of the Juno Mission. *Space Sci. Rev.*, *213*, 219-287. doi: 10.1007/s11214-014-0036-8

Bagenal, F., & Murdin, P. (2000, November). Planetary Magnetospheres. In *Encyclopedia of astronomy and astrophysics.* doi: 10.1888/0333750888/2322

Birn, J., Artemyev, A. V., Baker, D. N., Echim, M., Hoshino, M., & Zelenyi, L. M. (2012). Particle acceleration in the magnetotail and aurora. *Space Sci. Rev.*, *173*, 49-102. doi: 10.1007/s11214-012-9874-4

Birn, J., Dorelli, J. C., Hesse, M., & Schindler, K. (2004, February). Thin current sheets and loss of equilibrium: Three-dimensional theory and simulations. *J. Geophys. Res.*, *109*, 2215. doi: 10.1029/2003JA010275

Birn, J., Schindler, K., & Hesse, M. (2004, February). Thin electron current sheets and their relation to auroral potentials. *J. Geophys. Res.*, *109*, 2217. doi: 10.1029/2003JA010303

Chaston, C. C., Carlson, C. W., McFadden, J. P., Ergun, R. E., & Strangeway, R. J. (2007, April). How important are dispersive Alfvén waves for auroral particle acceleration? *Geophys. Res. Lett.*, *34*(7), L07101. doi: 10.1029/2006GL029144

Cheng, A. F. (1983, January). Thin, rotating plasma disks. *J. Geophys. Res.*, *88*, 13-18. doi: 10.1029/JA088iA01p00013

Clark, G., Mauk, B. H., Paranicas, C., Kollmann, P., & Smith, H. T. (2016, Mar). Charge states of energetic oxygen and sulfur ions in Jupiter's magnetosphere. *Journal of Geophysical Research (Space Physics)*, *121*(3), 2264-2273. doi: 10.1002/2015JA022257

Connerney, J. E. P., Acuña, M. H., Ness, N. F., & Satoh, T. (1998, Jun). New models of Jupiter's magnetic field constrained by the Io flux tube footprint. *J. Geophys. Res.*, *103*(A6), 11929-11940. doi: 10.1029/97JA03726

Connerney, J. E. P., Adriani, A., Allegrini, F., Bagenal, F., Bolton, S. J., Bonfond, B., . . . Waite, J. (2017, May). Jupiter's magnetosphere and aurorae observed by the Juno spacecraft during its first polar orbits. *Science*, *356*, 826-832. doi: 10.1126/science.aam5928

Connerney, J. E. P., Benn, M., Bjarno, J. B., Denver, T., Espley, J., Jorgensen, J. L., . . . Smith, E. J. (2017, November). The Juno Magnetic Field Investigation. *Space Sci. Rev.*, *213*, 39-138. doi: 10.1007/s11214-017-0334-z

Connerney, J. E. P., Timmins, S., Herceg, M., & Joergensen, J. L. (2020, Octo-

ber). A Jovian Magnetodisc Model for the Juno Era. *Journal of Geophysical Research (Space Physics)*, *125*(10), e28138. doi: 10.1029/2020JA028138

Cowley, S. W. H. (1978, November). The effect of pressure anisotropy on the equilibrium structure of magnetic current sheets. *Planetary and Space Science*, *26*, 1037-1061. doi: 10.1016/0032-0633(78)90028-4

Cowley, S. W. H., & Pellat, R. (1979, March). A note on adiabatic solutions of the one-dimensional current sheet problem. *Planatary Space Science*, *27*, 265-271. doi: 10.1016/0032-0633(79)90069-2

Damiano, P. A., Delamere, P. A., Stauffer, B., Ng, C. S., & Johnson, J. R. (2019, March). Kinetic Simulations of Electron Acceleration by Dispersive Scale Alfvén Waves in Jupiter's Magnetosphere. *Geophys. Res. Lett.*, *46*(6), 3043-3051. doi: 10.1029/2018GL081219

DiBraccio, G. A., Espley, J. R., Gruesbeck, J. R., Connerney, J. E. P., Brain, D. A., Halekas, J. S., ... Jakosky, B. M. (2015, November). Magnetotail dynamics at Mars: Initial MAVEN observations. *Geophys. Res. Lett.*, *42*, 8828-8837. doi: 10.1002/2015GL065248

Drake, J. F., & Lee, Y. C. (1977, August). Kinetic theory of tearing instabilities. *Physics of Fluids*, *20*, 1341-1353. doi: 10.1063/1.862017

Elliott, S. S., Gurnett, D. A., Yoon, P. H., Kurth, W. S., Mauk, B. H., Ebert, R. W., ... Sulaiman, A. H. (2020, June). The Generation of Upward-Propagating Whistler Mode Waves by Electron Beams in the Jovian Polar Regions. *Journal of Geophysical Research (Space Physics)*, *125*(6), e27868. doi: 10.1029/2020JA027868

Ergun, R. E., Andersson, L., Main, D., Su, Y. J., Newman, D. L., Goldman, M. V., ... Mozer, F. S. (2004, December). Auroral particle acceleration by strong double layers: The upward current region. *Journal of Geophysical Research (Space Physics)*, *109*(A12), A12220. doi: 10.1029/2004JA010545

Francfort, P., & Pellat, R. (1976, August). Magnetic merging in collisionless plasmas. *Geophys. Res. Lett.*, *3*, 433-436. doi: 10.1029/GL003i008p00433

Frank, L. A., Paterson, W. R., & Khurana, K. K. (2002, January). Observations of thermal plasmas in Jupiter's magnetotail. *J. Geophys. Res.*, *107*, 1003. doi: 10.1029/2001JA000077

Gonzalez, W., & Parker, E. (2016). *Magnetic Reconnection* (Vol. 427). doi: 10.1007/978-3-319-26432-5

Hada, T., Nishida, A., Terasawa, T., & Hones, E. W., Jr. (1981, December). Bi-directional electron pitch angle anisotropy in the plasma sheet. *J. Geophys. Res.*, *86*, 11211-11224. doi: 10.1029/JA086iA13p11211

Harrison, M. G., & Neukirch, T. (2009, February). Some remarks on one-dimensional force-free Vlasov-Maxwell equilibria. *Physics of Plasmas*, *16*(2), 022106. doi: 10.1063/1.3077307

Hau, L. N., & Voigt, G. H. (1992, June). Loss of MHD equilibrium caused by the enhancment of the magnetic B_y component in Earth's magnetotail. *J. Geophys. Res.*, *97*(A6), 8707-8711. doi: 10.1029/92JA00445

Hesse, M., Winske, D., & Birn, J. (1998, January). On the ion-scale structure of thin current sheets in the magnetotail. *Physica Scripta Volume T*, *74*, 63-66. doi: 10.1088/0031-8949/1998/T74/012

Hill, T. W. (1979, November). Inertial limit on corotation. *J. Geophys. Res.*, *84*, 6554-6558. doi: 10.1029/JA084iA11p06554

Hill, T. W., & Carbary, J. F. (1978, Dec). Centrifugal distortion of the Jovian magnetosphere by an equatorially confined current sheet. *J. Geophys. Res.*, *83*(A12), 5745-5749. doi: 10.1029/JA083iA12p05745

Hilmer, R. V., & Voigt, G. (1987, August). The effects of magnetic B(y) component on geomagnetic tail equilibria. *J. Geophys. Res.*, *92*, 8660-8672. doi: 10.1029/JA092iA08p08660

Hsieh, M.-S., & Otto, A. (2015, June). Thin current sheet formation in response

to the loading and the depletion of magnetic flux during the substorm growth phase. *J. Geophys. Res.*, *120*, 4264-4278. doi: 10.1002/2014JA020925

Hudson, P. D. (1970, November). Discontinuities in an anisotropic plasma and their identification in the solar wind. *Planatary Space Science*, *18*, 1611-1622. doi: 10.1016/0032-0633(70)90036-X

Huscher, E., Bagenal, F., Wilson, R. J., Allegrini, F., Ebert, R. W., Valek, P. W., . . . Levin, S. M. (2021, August). Survey of Juno Observations in Jupiter's Plasma Disk: Density. *Journal of Geophysical Research (Space Physics)*, *126*(8), e29446. doi: 10.1029/2021JA029446

Jackman, C. M., Arridge, C. S., André, N., Bagenal, F., Birn, J., Freeman, M. P., . . . Walsh, A. P. (2014, August). Large-Scale Structure and Dynamics of the Magnetotails of Mercury, Earth, Jupiter and Saturn. *Space Sci. Rev.*, *182*, 85-154. doi: 10.1007/s11214-014-0060-8

Kamaletdinov, S. R., Yushkov, E. V., Artemyev, A. V., Lukin, A. S., & Vasko, I. Y. (2020, August). Superthin current sheets supported by anisotropic electrons. *Physics of Plasmas*, *27*(8), 082904. doi: 10.1063/5.0018063

Kane, M., Williams, D. J., Mauk, B. H., McEntire, R. W., & Roelof, E. C. (1999, January). Galileo Energetic Particles Detector measurements of hot ions in the neutral sheet region of Jupiter's magnetodisk. *Geophys. Res. Lett.*, *26*, 5-8. doi: 10.1029/1998GL900267

Khurana, K. K., Kivelson, M. G., Vasyliunas, V. M., Krupp, N., Woch, J., Lagg, A., . . . Kurth, W. S. (2004). The configuration of Jupiter's magnetosphere. In F. Bagenal, T. E. Dowling, & W. B. McKinnon (Eds.), *Jupiter. the planet, satellites and magnetosphere* (p. 593-616).

Khurana, K. K., Leinweber, H. K., Hospodarsky, G. B., & Paranicas, C. P. (2022). Radial and local time variations in the thickness of jupiter's magnetospheric current sheet. *Journal of Geophysical Research: Space Physics*, *127*(10), e2022JA030664. doi: doi:10.1029/2022JA030664

Khurana, K. K., & Liu, J. (2018, March). Current Systems in Planetary Magnetospheres: A Comparative Overview. In A. Keiling, O. Marghitu, & M. Wheatland (Eds.), *Electric currents in geospace and beyond* (Vol. 235, p. 17-41). doi: 10.1002/9781119324522.ch2

Khurana, K. K., & Schwarzl, H. K. (2005, July). Global structure of Jupiter's magnetospheric current sheet. *J. Geophys. Res.*, *110*, 7227. doi: 10.1029/2004JA010757

Kim, T. K., Ebert, R. W., Valek, P. W., Allegrini, F., McComas, D. J., Bagenal, F., . . . Nicolaou, G. (2020a, February). Method to Derive Ion Properties From Juno JADE Including Abundance Estimates for O^+ and S^{2+}. *Journal of Geophysical Research (Space Physics)*, *125*(2), e26169. doi: 10.1029/2018JA026169

Kim, T. K., Ebert, R. W., Valek, P. W., Allegrini, F., McComas, D. J., Bagenal, F., . . . Bolton, S. J. (2020b, April). Survey of Ion Properties in Jupiter's Plasma Sheet: Juno JADE-I Observations. *Journal of Geophysical Research (Space Physics)*, *125*(4), e27696. doi: 10.1029/2019JA027696

Kollmann, P., Roussos, E., Paranicas, C., Woodfield, E. E., Mauk, B. H., Clark, G., . . . Vandegriff, J. (2018, November). Electron Acceleration to MeV Energies at Jupiter and Saturn. *Journal of Geophysical Research (Space Physics)*, *123*(11), 9110-9129. doi: 10.1029/2018JA025665

Kronberg, E. A., Kasahara, S., Krupp, N., & Woch, J. (2012, January). Field-aligned beams and reconnection in the jovian magnetotail. *Icarus*, *217*, 55-65. doi: 10.1016/j.icarus.2011.10.011

Krupp, N., Woch, J., Lagg, A., Livi, S., Mitchell, D. G., Krimigis, S. M., . . . Espinosa, S. A. (2004, Sep). Energetic particle observations in the vicinity of Jupiter: Cassini MIMI/LEMMS results. *Journal of Geophysical Research (Space Physics)*, *109*(A9), A09S10. doi: 10.1029/2003JA010111

Liu, Z. Y., Zong, Q. G., Blanc, M., Sun, Y. X., Zhao, J. T., Hao, Y. X., & Mauk, B. H. (2021, November). Statistics on Jupiter's Current Sheet With Juno Data: Geometry, Magnetic Fields and Energetic Particles. *Journal of Geophysical Research (Space Physics)*, *126*(11), e29710. doi: 10.1029/2021JA029710

Lu, S., Artemyev, A. V., Angelopoulos, V., Lin, Y., Zhang, X. J., Liu, J., ... Strangeway, R. J. (2019, Feb). The Hall Electric Field in Earth's Magnetotail Thin Current Sheet. *Journal of Geophysical Research (Space Physics)*, *124*(2), 1052-1062. doi: 10.1029/2018JA026202

Lu, S., Lin, Y., Angelopoulos, V., Artemyev, A. V., Pritchett, P. L., Lu, Q., & Wang, X. Y. (2016, December). Hall effect control of magnetotail dawn-dusk asymmetry: A three-dimensional global hybrid simulation. *J. Geophys. Res.*, *121*, 11. doi: 10.1002/2016JA023325

Lukin, A. S., Vasko, I., Artemyev, A., & Yushkov, E. (2018, January). Two-dimensional self-similar plasma equilibria. *Physics of Plasmas*, *25*(1), 012906. doi: 10.1063/1.5016178

Lysak, R. L., Song, Y., Elliott, S., Kurth, W., Sulaiman, A. H., & Gershman, D. (2021, December). The Jovian Ionospheric Alfvén Resonator and Auroral Particle Acceleration. *Journal of Geophysical Research (Space Physics)*, *126*(12), e29886. doi: 10.1029/2021JA029886

Mauk, B. H., Clark, G., Gladstone, G. R., Kotsiaros, S., Adriani, A., Allegrini, F., ... Rymer, A. M. (2020, March). Energetic Particles and Acceleration Regions Over Jupiter's Polar Cap and Main Aurora: A Broad Overview. *Journal of Geophysical Research (Space Physics)*, *125*(3), e27699. doi: 10.1029/2019JA027699

Mauk, B. H., Haggerty, D. K., Paranicas, C., Clark, G., Kollmann, P., Rymer, A. M., ... Valek, P. (2017a, September). Discrete and broadband electron acceleration in Jupiter's powerful aurora. *Nature*, *549*(7670), 66-69. doi: 10.1038/nature23648

Mauk, B. H., Haggerty, D. K., Paranicas, C., Clark, G., Kollmann, P., Rymer, A. M., ... Valek, P. (2017b, May). Juno observations of energetic charged particles over Jupiter's polar regions: Analysis of monodirectional and bidirectional electron beams. *Geophys. Res. Lett.*, *44*, 4410-4418. doi: 10.1002/2016GL072286

Mauk, B. H., Mitchell, D. G., McEntire, R. W., Paranicas, C. P., Roelof, E. C., Williams, D. J., ... Lagg, A. (2004, July). Energetic ion characteristics and neutral gas interactions in Jupiter's magnetosphere. *J. Geophys. Res.*, *109*, 9. doi: 10.1029/2003JA010270

McComas, D. J., Alexander, N., Allegrini, F., Bagenal, F., Beebe, C., Clark, G., ... White, D. (2017, November). The Jovian Auroral Distributions Experiment (JADE) on the Juno Mission to Jupiter. *Space Sci. Rev.*, *213*, 547-643. doi: 10.1007/s11214-013-9990-9

McComas, D. J., Szalay, J. R., Allegrini, F., Bagenal, F., Connerney, J., Ebert, R. W., ... Bolton, S. (2017, May). Plasma environment at the dawn flank of Jupiter's magnetosphere: Juno arrives at Jupiter. *Geophys. Res. Lett.*, *44*, 4432-4438. doi: 10.1002/2017GL072831

Mingalev, O. V., Malova, H. V., Mingalev, I. V., Mel'nik, M. N., Setsko, P. V., & Zelenyi, L. M. (2018, October). Model of a Thin Current Sheet in the Earth's Magnetotail with a Kinetic Description of Magnetized Electrons. *Plasma Physics Reports*, *44*(10), 899-919. doi: 10.1134/S1063780X18100082

Mingalev, O. V., Mingalev, I. V., Mel'nik, M. N., Artemyev, A. V., Malova, H. V., Popov, V. Y., ... Zelenyi, L. M. (2012, April). Kinetic models of current sheets with a sheared magnetic field. *Plasma Physics Reports*, *38*, 300-314. doi: 10.1134/S1063780X12030063

Nakamura, R., Baumjohann, W., Fujimoto, M., Asano, Y., Runov, A., Owen, C. J., ... Khotyaintsev, Y. (2008, April). Cluster observations of an ion-scale current

sheet in the magnetotail under the presence of a guide field. *J. Geophys. Res.*, *113*, 7. doi: 10.1029/2007JA012760

Neukirch, T., Vasko, I. Y., Artemyev, A. V., & Allanson, O. (2020, March). Kinetic Models of Tangential Discontinuities in the Solar Wind. *Astrophys. J.*, *891*(1), 86. doi: 10.3847/1538-4357/ab7234

Neukirch, T., Wilson, F., & Allanson, O. (2020, June). . *Journal of Plasma Physics*, *86*(3), 825860302. doi: 10.1017/S0022377820000604

Panov, E. V., Artemyev, A. V., Nakamura, R., & Baumjohann, W. (2011). Two Types of Tangential Magnetopause Current Sheets: Cluster Observations and Theory. *J. Geophys. Res.*, *116*, A12204. doi: 10.1029/2011JA016860

Petrukovich, A. A., Baumjohann, W., Nakamura, R., Runov, A., Balogh, A., & Rème, H. (2007, October). Thinning and stretching of the plasma sheet. *J. Geophys. Res.*, *112*, 10213. doi: 10.1029/2007JA012349

Rich, F. J., Vasyliunas, V. M., & Wolf, R. A. (1972). On the Balance of Stresses in the Plasma Sheet. *J. Geophys. Res.*, *77*, 4670-4676. doi: 10.1029/JA077i025p04670

Rong, Z. J., Barabash, S., Stenberg, G., Futaana, Y., Zhang, T. L., Wan, W. X., . . . Zhong, J. (2015, July). The flapping motion of the Venusian magnetotail: Venus Express observations. *J. Geophys. Res.*, *120*, 5593-5602. doi: 10.1002/2015JA021317

Runov, A., Sergeev, V. A., Nakamura, R., Baumjohann, W., Apatenkov, S., Asano, Y., . . . Balogh, A. (2006, March). Local structure of the magnetotail current sheet: 2001 Cluster observations. *Annales Geophysicae*, *24*, 247-262.

Saur, J., Janser, S., Schreiner, A., Clark, G., Mauk, B. H., Kollmann, P., . . . Kotsiaros, S. (2018, November). Wave-Particle Interaction of Alfvén Waves in Jupiter's Magnetosphere: Auroral and Magnetospheric Particle Acceleration. *Journal of Geophysical Research (Space Physics)*, *123*(11), 9560-9573. doi: 10.1029/2018JA025948

Schindler, K., & Birn, J. (2002, August). Models of two-dimensional embedded thin current sheets from Vlasov theory. *J. Geophys. Res.*, *107*, 1193. doi: 10.1029/2001JA000304

Schindler, K., Birn, J., & Hesse, M. (2012, August). Kinetic model of electric potentials in localized collisionless plasma structures under steady quasi-gyrotropic conditions. *Physics of Plasmas*, *19*(8), 082904. doi: 10.1063/1.4747162

Selesnick, R. S., & Cohen, C. M. S. (2009, Jan). Charge states of energetic ions in Jupiter's radiation belt inferred from absorption microsignatures of Io. *Journal of Geophysical Research (Space Physics)*, *114*(A1), A01207. doi: 10.1029/2008JA013722

Shkarofsky, I. P., Johnston, T. W., & Bachnynski, M. P. (1966). *The particle kinetic of plasmas.* Addison-wesley Piblishing company.

Sitnov, M. I., Birn, J., Ferdousi, B., Gordeev, E., Khotyaintsev, Y., Merkin, V., . . . Zhou, X. (2019, Jun). Explosive Magnetotail Activity. *Space Sci. Rev.*, *215*(4), 31. doi: 10.1007/s11214-019-0599-5

Sitnov, M. I., & Merkin, V. G. (2016, August). Generalized magnetotail equilibria: Effects of the dipole field, thin current sheets, and magnetic flux accumulation. *J. Geophys. Res.*, *121*, 7664-7683. doi: 10.1002/2016JA023001

Sitnov, M. I., Swisdak, M., Guzdar, P. N., & Runov, A. (2006, August). Structure and dynamics of a new class of thin current sheets. *J. Geophys. Res.*, *111*, 8204. doi: 10.1029/2005JA011517

Sonnerup, B. U. Ö., & Cahill, L. J., Jr. (1968, March). Explorer 12 observations of the magnetopause current layer. *J. Geophys. Res.*, *73*, 1757. doi: 10.1029/JA073i005p01757

Sonnerup, B. U. Ö., & Su, S.-Y. (1967, February). Large Amplitude Whistler Waves in a Hot Collision-Free Plasma. *Physics of Fluids*, *10*, 462-464. doi: 10.1063/1.1762132

Syrovatskii, S. I. (1981). Pinch sheets and reconnection in astrophysics. *Annual review of astronomy and astrophysics*, *19*, 163-229. doi: 10.1146/annurev.aa.19.090181.001115

Thomas, N., Bagenal, F., Hill, T. W., & Wilson, J. K. (2004). The Io neutral clouds and plasma torus. In F. Bagenal, T. E. Dowling, & W. B. McKinnon (Eds.), *Jupiter. the planet, satellites and magnetosphere* (Vol. 1, p. 561-591).

Vasko, I. Y., Artemyev, A. V., Petrukovich, A. A., & Malova, H. V. (2014). Thin current sheets with strong bell-shape guide field: Cluster observations and models with beams. *Annales Geophysicae*, *32*(10), 1349–1360. Retrieved from http://www.ann-geophys.net/32/1349/2014/ doi: 10.5194/angeo-32-1349-2014

Vasko, I. Y., Artemyev, A. V., Popov, V. Y., & Malova, H. V. (2013, February). Kinetic models of two-dimensional plane and axially symmetric current sheets: Group theory approach. *Physics of Plasmas*, *20*(2), 022110. doi: 10.1063/1.4792263

Waldrop, L. S., Fritz, T. A., Kivelson, M. G., Khurana, K., Krupp, N., & Lagg, A. (2005, May). Jovian plasma sheet morphology: particle and field observations by the Galileo spacecraft. *Planatary Space Science*, *53*, 681-692. doi: 10.1016/j.pss.2004.11.003

Walsh, A. P., Fazakerley, A. N., Forsyth, C., Owen, C. J., Taylor, M. G. G. T., & Rae, I. J. (2013). Sources of electron pitch angle anisotropy in the magnetotail plasma sheet. *J. Geophys. Res.*, *118*, 6042–6054. doi: 10.1002/jgra.50553

Watt, C. E. J., & Rankin, R. (2009, January). Electron Trapping in Shear Alfvén Waves that Power the Aurora. *Physical Review Letters*, *102*(4), 045002. doi: 10.1103/PhysRevLett.102.045002

Wilson, F., Neukirch, T., Hesse, M., Harrison, M. G., & Stark, C. R. (2016, March). Particle-in-cell simulations of collisionless magnetic reconnection with a non-uniform guide field. *Physics of Plasmas*, *23*(3), 032302. doi: 10.1063/1.4942939

Xu, S., Runov, A., Artemyev, A., Angelopoulos, V., & Lu, Q. (2018, May). Intense Cross-Tail Field-Aligned Currents in the Plasma Sheet at Lunar Distances. *Geophys. Res. Lett.*, *45*, 4610-4617. doi: 10.1029/2018GL077902

Yoon, P. H., & Lui, A. T. Y. (2005, January). A class of exact two-dimensional kinetic current sheet equilibria. *J. Geophys. Res.*, *110*, 1202. doi: 10.1029/2003JA010308

Yoon, Y. D., Yun, G. S., Wendel, D. E., & Burch, J. L. (2021, January). Collisionless relaxation of a disequilibrated current sheet and implications for bifurcated structures. *Nature Communications*, *12*, 3774. doi: 10.1038/s41467-021-24006-x

Zelenyi, L. M., Artemyev, A. V., & Petrukovich, A. A. (2010, March). Earthward electric field in the magnetotail: Cluster observations and theoretical estimates. *Geophys. Res. Lett.*, *37*, 6105. doi: 10.1029/2009GL042099

Zelenyi, L. M., Malova, H. V., Artemyev, A. V., Popov, V. Y., & Petrukovich, A. A. (2011, February). Thin current sheets in collisionless plasma: Equilibrium structure, plasma instabilities, and particle acceleration. *Plasma Physics Reports*, *37*, 118-160. doi: 10.1134/S1063780X1102005X

Zelenyi, L. M., Malova, H. V., Leonenko, M. V., Grigorenko, E. E., & Popov, V. Y. (2022). Equilibrium configurations of super-thin current sheets in space plasma: Characteristic scaling of multilayer structures. *Journal of Geophysical Research (Space Physics)*, *127*, e2022JA030881. doi: 10.1029/2022JA030881

Zelenyi, L. M., Malova, H. V., Popov, V. Y., Delcourt, D., & Sharma, A. S. (2004, November). Nonlinear equilibrium structure of thin currents sheets: influence of electron pressure anisotropy. *Nonlinear Processes in Geophysics*, *11*, 579-587.

Zelenyi, L. M., & Taktakishvili, A. L. (1987, June). Spontaneous magnetic reconnec-

tion mechanisms in plasma. *Astrophysics and Space Science*, *134*, 185-196. doi: 10.1007/BF00636466

Zhang, X. J., Ma, Q., Artemyev, A. V., Li, W., Kurth, W. S., Mauk, B. H., ... Bolton, S. J.   (2020, August).   Plasma Sheet Boundary Layer in Jupiter's Magnetodisk as Observed by Juno.   *Journal of Geophysical Research (Space Physics)*, *125*(8), e27957. doi: 10.1029/2020JA027957

Zimbardo, G.   (1989, July).   A self-consistent picture of Jupiter's nightside magneto-sphere.   *J. Geophys. Res.*, *94*, 8707-8719. doi: 10.1029/JA094iA07p08707